

Muñoz-Salinas, E., Castillo, M., Sanderson, D., Kinnaird, T., and Cruz-Zaragoza, E. (2016) Using three different approaches of OSL for the study of young fluvial sediments at the coastal plain of the Usumacinta–Grijalva River Basin, southern Mexico. *Earth Surface Processes and Landforms*, 41(6), pp. 823-834. (doi:[10.1002/esp.3880](https://doi.org/10.1002/esp.3880))

This is the author's final accepted version.

There may be differences between this version and the published version. You are advised to consult the publisher's version if you wish to cite from it.

<http://eprints.gla.ac.uk/132700/>

Deposited on: 22 November 2016

1                   1   **Using three different approaches of OSL for the study of**  
2                   2   **young fluvial sediments at the coastal plain of the**  
3                   3   **Usumacinta–Grijalva River Basin, Southern Mexico**

4  
5                   5   *Muñoz-Salinas, E.<sup>1\*</sup>, Castillo, M.<sup>1</sup>, Sanderson, D.<sup>2</sup>, Kinnaird, T.<sup>2</sup>, Cruz-*  
6                   6   *Zaragoza, E.<sup>3</sup>*

7  
8                   8   <sup>1</sup> Instituto de Geología, Universidad Nacional Autónoma de México, UNAM,  
9                   9   Mexico, Mexico

10                  2   <sup>2</sup> Scottish Universities Environmental Research Centre, SUERC, Glasgow, UK

11                  3   <sup>3</sup> Instituto de Ciencias Nucleares, Universidad Nacional Autónoma de México,  
12                  UNAM, Mexico, Mexico

13                  \* Correspondence author. Email: emsalinas@geologia.unam.mx

14  
15   **ABSTRACT:** We use three different approaches of optically stimulated  
16   luminescence (OSL) to study young fluvial sediments located at the main  
17   channels of one of the largest fluvial systems of North America: the  
18   Usumacinta–Grijalva. We use the Pulsed Photo-Stimulated Luminescence  
19   (PPSL) system also known as portable OSL reader, full OSL dating and  
20   profiling OSL dating in samples extracted from vertical sediment profiles ( $n =$   
21   9) of riverbanks to detect changes in depositional rates of sediments and to  
22   obtain the age of the deposits. The results of the PPSL system show that the  
23   luminescence signals of vertical sediment profiles highly scattered from the top  
24   to the bottom contrast with the luminescence pattern observed on well–reset  
25   sequences of fluvial deposits where luminescence increase from the top to the

bottom of the profile. The profiling and full OSL ages yielded large uncertainty values on their ages. Based on the inconsistencies observed in both ages and luminescence patterns of profiles we suggest that these fluvial deposits were not fully reset during their transport. As an explanation, we propose that in the Usumacinta and Grijalva rivers the cyclonic storms during the wet season promote the entrainment of large volumes of sediments due to high-erosional episodes around the basin resulting from hyper-concentrated and turbid flows. We conclude that the PPSL, profiling and full OSL dating of sediments are useful tools to quantify and to assess the depositional patterns in fluvial settings during the Holocene. These techniques also can yield information about sites where increases in the sediment load of rivers may produce poorly resetting of grains affecting the results of OSL dating.

**Keywords:** Fluvial sediments; OSL; PPSL system (portable OSL reader); Usumacinta–Grijalva River Basin; Mexico

## Introduction

The optically stimulated luminescence (OSL) technique is based on the study of the luminescence emitted by mineral grains after their optical stimulation. Luminescence signals are measured in photons and result from the electromagnetic energy released when excited electrons trapped within imperfections of grain lattices or traps in the gap band return to less energetic positions of the valence band (Aitken, 1995). The process described occurs when grains are exposed to visible, or nearly close to visible wavelengths of

the electromagnetic spectrum or when grains are heated to temperatures higher than 400 °C.

In ideal situations for OSL dating, grains must be fully exposed to sunlight during their transport by air, water, and gravity or the grains may become heated at high temperatures. Under these conditions the electrons located at the traps return to the valence band. These grains become “reset”, or in other words, the clock is set to zero prior to their burial. It is during the burial time when natural radiation of sediments and/or soils causes the trapping of electrons within mineral grains producing the “charging” of grains with luminescence (Aitken, 1995; 1998). Thus, in a vertical sediment profile containing a sequence of well-reset deposits, where the oldest deposits are at the base of the profile and the youngest are on the top, the pattern of luminescence signals steadily decreases from the bottom to the top of the profile.

The pattern of luminescence previously described is common in some fluvial-dominated landscapes. Lomax et al., (2007) found that palaeodoses increase with depth in a profile of 4 m of sediments extracted from an aeolian dominated environment located at the western sector of the Murray River Basin, Australia. Muñoz-Salinas et al., (2011; 2014) and Portenga and Bishop (2015) reported a case in the Lachlan River, Australia (see Fig. 1A), where the sediments sampled at the bottom of the profile contained more luminescence than those extracted from the top of the profile. Usually, in settings where sediments are well-reset, most of the equivalent doses from different aliquots,

1  
2  
3 76 which are needed for the full OSL dating, are within 2 standard deviations  
4  
5 77 (Duller, 2008). This low scatter is shown in the case of the samples WEH1-1,  
6  
7 78 WEH2-1 and WEH2-3 analysed in the work of Kunk et al., (2013). These  
8  
9  
10 79 samples were extracted from the fluvial deposits of one of the major rivers of  
11  
12 80 Europe, the Elbe River in Northern Germany. For the case of the Lachlan  
13  
14 81 River, Muñoz-Salinas et al., (2011; 2014) calculated an age with uncertainty of  
15  
16 82  $2.43 \pm 0.14$  ka (SUTL2356) (see Fig. 2A).  
17

18  
19  
20  
21 84 There are sedimentary processes in which the luminescence signals in  
22  
23 85 mineral grains deviate from the ideal situations previously described. This  
24  
25 86 happens when the grains have not been completely exposed to sunlight during  
26  
27 87 their transport resulting in a partially bleaching of these with some electrons  
28  
29 88 remaining in their traps. In this case the grains are poorly reset and they  
30  
31 89 contain an “inherited luminescence”. This process has been inferred from  
32  
33 90 fluvial sediments of different sites (e.g., Galbraith et al., 1999; Duller, 2004;  
34  
35 91 Brook et al., 2006). In this case, the inherited luminescence is stored in the  
36  
37 92 grains and is subsequently added to next processes of electron trapping  
38  
39 93 (Aitken, 1995; 1998; Singarayer et al., 2005). If the conditions described above  
40  
41 94 predominate, the OSL age is overestimated (Duller, 2008).  
42  
43  
44

45  
46  
47 96 In sites where mineral grains have not been fully reset, it is expected that the  
48  
49 97 trend of the luminescence signals within a vertical sediment profile exhibit a  
50  
51 98 weak correlation with depth or no correlation at all. This is the case analysed  
52  
53 99 by Stang et al., (2012) in three vertical soil profiles of ~ 30 cm depth extracted  
54  
55  
56  
57  
58  
59  
60

100 from poorly-sorted deposits that came from the denudation of a granitic  
101 batholith at San Gabriel Mountains, southern California, USA.

102

103 In an archaeological site located in cava Petrini, southern Italy, Sanderson and  
104 Murphy (2010) found that luminescence signals decrease with depth in a  
105 vertical sediment profile. This last case is unexpected because the oldest  
106 sediments are found as depth increases. The profile that these authors studied  
107 contained deposits transported by two different geomorphic processes: (1)  
108 rapid mass movement at the top between ~0-150 cm depth and (2) long-term  
109 soil development at the bottom between ~150-300 cm depth. Another case, in  
110 a lahar deposit resulting from a hyper-concentrated flow at the Popocatepetl  
111 volcano in central Mexico, Muñoz-Salinas et al., (2011) reported a random  
112 pattern of luminescence signals along a vertical sediment profile (see Fig. 1B).

113

114 In the case of poorly reset deposits, the equivalent doses of most of the  
115 aliquots are beyond 2 standard deviations (Duller, 2008). Therefore, errors are  
116 high for age values that end up being the OSL estimate. In a debris flow  
117 deposit in Gredos Gorge, central Spain, Muñoz-Salinas et al., (2013) reported  
118 an age and uncertainty of  $10.7 \pm 1.6$  ka (SUTL2351; see Fig. 2B). For the case  
119 of Gredos, the uncertainty in the age of the deposit is considerable higher (1.6  
120 ka) than the one calculated for the well-reset deposits studied at Lachlan River  
121 (i.e. sample: SUTL2356, uncertainty 140 years) (Muñoz-Salinas et al., 2013).

122

123 The examples cited above suggest that the luminescence of sediments may  
124 change according to the type of sediment transport. In this paper we study the

125 fluvial sediments of the Usumacinta and Grijalva rivers that together compose  
126 one of the largest fluvial systems of North America. We focus on the  
127 assessment of the fluvial deposits of the Holocene found at the margins of the  
128 main channel of rivers, in order to understand the recent sedimentation pattern  
129 and assuming that, because the setting corresponds to a fluvial-dominated  
130 landscape, the grains are probably well-reset like those previously described  
131 for the ideal situations for OSL dating (see Fig. 1A and 2A). Our assumption of  
132 finding well-reset grains for the young fluvial deposits of Usumacinta and  
133 Grijalva rivers in the floodplain is based on the hypothesis that (1) the grains  
134 may have been fully exposed to sunlight during their transport because there  
135 is a large distance from the headwaters to the floodplain and (2) since in  
136 tropical landscapes the sunlight exposure is high for long hours and there are  
137 high rates of solar radiation, the grains are likely to be set to zero prior to their  
138 burial time.

140 In this study we exploited the OSL technique using three different approaches:  
141 (1) the application of a Pulsed Photo-Stimulated Luminescence (PPSL)  
142 system, also known as portable OSL reader, (2) the full OSL dating and (3) the  
143 profiling OSL method. We use these three methods because these  
144 approaches allow (1) the dating of recent fluvial sediments and (2) the analysis  
145 of sediment transport based on the study of luminescence signals.

## 147 **Study area**

1  
2  
3 149 The rivers Usumacinta and Grijalva form a single river basin, however each  
4  
5 150 river flows separately before joining just ~15 km off the coast of the Gulf of  
6  
7 151 Mexico (Fig. 3). The headwater of each of the two rivers is located in  
8  
9 152 Guatemala (Hudson et al., 2005) and they mostly flow in the southern part of  
10  
11 153 Mexico, crossing the States of Chiapas and Tabasco. The Grijalva River has a  
12  
13 154 total length of ~640 km and the Usumacinta River is ~1100 km (Day et al.,  
14  
15 155 2003). The Usumancinta and Grijalva river basin (UGRB) is the largest fluvial  
16  
17 156 system of Mexico and it is placed in the number 10<sup>th</sup> of the ranking of the  
18  
19 157 major rivers of North America (Benke, 2009). The total discharge of the UGRB  
20  
21 158 is ~2,678 m<sup>3</sup>s<sup>-1</sup> and its basin area is of ~112,000 km<sup>2</sup> (Benke, 2009).  
22  
23  
24  
25  
26

27 160 Two main geomorphological units characterize the UGRB: (1) The coastal  
28  
29 161 plain located at the lowlands and (2) the mountain area located at the  
30  
31 162 highlands (Hudson et al., 2005) (Fig. 3). In the first unit a low relief area  
32  
33 163 consisting of wetlands forms the wide coastal plain of the Gulf of Mexico  
34  
35 164 (Benke, 2009) and extends from the coast to ~120 km inland. The main  
36  
37 165 lithology of this geomorphic unit is Cenozoic sediments and rocks. The  
38  
39 166 sediments result from the denudation of the mountainous area. Along the  
40  
41 167 coastal plain, the rivers have high sinuosity and the formation of meanders,  
42  
43 168 oxbox lakes, and chute channels is common.  
44  
45  
46

47 169  
48  
49 170 The second geomorphic unit is the mountain area which is composed by the  
50  
51 171 Sierra de los Cuchumatanes, the Sierra Madre de Chiapas and the Altos de  
52  
53 172 Chiapas. Between the Sierra Madre de Chiapas and the Altos de Chiapas it is  
54  
55 173 the Depresión Central de Chiapas, which is a large karstic canyon of ~600 m  
56  
57  
58  
59  
60



174 a.s.l. where the Grijalva River flows into (Fig. 3A). Cretaceous limestones and  
175 dolomites compose most of the Sierra de los Cuchumatanes (Marshall, 2007).  
176 The lithology of Sierra Madre de Chiapas is composed of diorites and granites  
177 belonging to a Paleozoic batholith (Cros et al., 1998; Morán-Zenteno et al.,  
178 1999). The Altos de Chiapas are constituted by Mesozoic sequences of  
179 marine and continental clastic–carbonate materials with the presence of some  
180 Cenozoic volcanic deposits (Morán-Zenteno et al., 1999) (Fig. 3B).

181  
182 The mean annual rainfall in the UGRB exceeds 2 m. The high rates of rainfall  
183 in this region influence the water discharge around the basin producing large  
184 water and sediment discharge rates (Hudson et al., 2005; Muñoz-Salinas et  
185 al., 2015). Nevertheless, the spatial distribution of rainfall is highly variable in  
186 the UGRB. The climate in the lowlands and part of the Altos de Chiapas is  
187 tropical without the presence of a dry season (<http://www.inegi.gob.mx>, 2013).  
188 In the highlands some areas receive more than 6 m of mean annual rainfall  
189 (<http://www.conagua.gob.mx>, 2013). The Inter-Tropical Convergence Zone  
190 generates an intense rainfall season that starts in May and ends in October.  
191 The drier season takes place from November to April (Grodsky and Carton,  
192 2003). At the UGRB, convective clouds and tropical cyclones prevail during  
193 the summer season. The heavy rainfalls produce the rapid increase in water  
194 discharges at the Usumacinta and Grijalva rivers causing the flooding of the  
195 lowlands (Rosengaus-Moshinsky et al., 2002).

196  
197 The distribution of the vegetation in the UGRB is controlled by the topographic  
198 gradient, which in turn, is related to the amount of rainfall and changes in

199 temperature gradient. The rapid change of elevation in just a few kilometers  
200 produces contrasting biophysical sites (Weibel, 1998). The main Eco–regions  
201 in the basin are composed by mangrove swamps and marshes in the coastal  
202 plain of the lowlands (Reyes et al., 2004) and tropical to subtropical forest in  
203 the highlands (Hudson et al, 2005; Ramírez-Marcial et al., 2001).

204

205 The UGRB has a long history of occupation that can be traced back to the  
206 Olmec Civilization that started around the 18<sup>th</sup> Century B.C. (Hirth et al., 2013).  
207 After the Olmecs, the Maya Civilization developed a complex system of land  
208 occupation during the Classic Period, which started from the 3<sup>rd</sup> Century B.C.  
209 and ended in the 9<sup>th</sup> Century A.D. After the collapse of the Maya Empire, the  
210 environment of the UGRB was slightly modified until the 20<sup>th</sup> Century  
211 (Zebadua, 1999), when deforestation rates around the UGRB became one of  
212 the highest around the world (Benjamin, 1981; Ochoa-Gaona and González-  
213 Espinosa, 2000).

214

215 The control of the water flow of the Grijalva River started in 1964 A.D. with the  
216 construction of the Netzahualcóyotl dam, which is the second largest dam of  
217 Mexico; capturing  $10 \times 10^4 \text{ m}^3$  of fresh water. The Belisario Dominguez dam  
218 was build in 1978, also in the Grijalva River, and captures  $15 \times 10^4 \text{ m}^3$  of fresh  
219 water, being the largest dam of Mexico (<http://www.conagua.gob.mx>, 2013).

220 The Usumacinta River is undammed.

221

222 **Methodology**

223

224 We use the PPSL unit, which has been recently proposed in the study of  
225 fluvial processes (Sanderson and Murphy, 2010; Muñoz-Salinas et al, 2011),  
226 to compare the luminescence signals of nine vertical sediment profiles  
227 extracted at the floodplains of the Usumacinta and Grijalva rivers with the ideal  
228 trend of well-reset deposits previously described. The goal is to assess if the  
229 grains of the fluvial deposits in these two rivers are well-reset, as hypothesized  
230 (Fig. 3) and, therefore, OSL can be used to establish a chronology of recent  
231 fluvial events.

232

233 The full OSL dating method is based in the conventional OSL dating protocol  
234 that use the Single-Aliquot Regenerative (SAR) method, which is used here in  
235 order to obtain the age of deposits selected at different depths of four different  
236 profiles. The profiling OSL dating is less accurate than the full OSL dating to  
237 obtain ages in sediments, in which only the equivalent doses are calculated for  
238 the samples. The dose rates in the profiling OSL dating are estimated from  
239 sites adjacent to the full OSL dating sites. In the profiling dating it is assumed  
240 that the sediment has similar radiation dosimetry than the sediment sampled  
241 for the full OSL dating method. We performed the profiling OSL at different  
242 depths of the four profiles selected to for the full OSL dating, since the dose  
243 rates calculated for the later are also used for the profiling.

244

245 Sample extraction during fieldwork

246

247 The samples analysed in this study were extracted at different depths of  
248 profiles composed by the deposits abandoned by the Usumacinta and Grijalva

249 rivers during the flooding of the overbanks. The sequence of these flood  
250 deposits can be recognized in the slopes located at the inner part of the main  
251 channel of the rivers, just where the water flow is regularly confined into the  
252 channel during the low flow stage. During the wet season, the water flow  
253 eventually raises above the main channel and inundates the overbanks. When  
254 this last situation of high flow stage takes place, the sediment transported by  
255 rivers is deposited on the surface of the overbanks and therefore, the  
256 overbanks contain valuable information about the most recent flood events  
257 (Fig. 4). The vertical sediment profiles in this study were selected only at the  
258 erosive margins of channels in order to avoid the sampling of the sediment  
259 remobilized by slope slides at the depositional margins (Fig. 4). Moreover, we  
260 avoided the sites with any visible sign of bioturbation caused by either animals  
261 or humans. To obtain the samples we performed two fieldwork campaigns that  
262 were carried out during the winter season (the first one in April 2012 and the  
263 second one in February 2013).

264  
265 We sampled a total of nine profiles, five at the Usumacinta River named  
266 USU1, USU2, USU3, USU13-1 and USU13-2, and four at the Grijalva River,  
267 coded GRIJ-PA1, GRIJ-PA2, GRIJ-PB1 and GRIJ-PB2. In all of the nine  
268 profiles we extracted samples for measuring the luminescence using the PPSL  
269 approach. We extracted samples for full OSL dating and OSL profiling in only  
270 three profiles of the Usumacinta River (USU2, USU13-1 and USU13-2) and in  
271 one profile of the Grijalva River (GRIJ-PA1; Fig. 5).

272

1  
2  
3 273 We performed the sampling of profiles during daylight. In order to prevent the  
4  
5 274 bleaching of the material during its extraction, we covered the profiles with a  
6  
7 275 thick black plastic cloth to darken the surface of the profile. Once covered the  
8  
9 276 surface, we introduced ourselves underneath the cloth and we removed ~5  
10  
11 277 mm of the outer material of the profile to avoid the sampling of sediment  
12  
13 278 exposed to sunlight. Next, we placed a measure tape oriented from top to  
14  
15 279 bottom next to the profile in order to reference the depths from the top where  
16  
17 280 samples were extracted. For the PPSL and the profiling OSL dating, samples  
18  
19 281 were extracted using pvc cylinders of ~3 cm long with ~1 cm of diameter and  
20  
21 282 for the full OSL dating we used pvc cylinders of ~20 cm long and ~5 cm of  
22  
23 283 diameter. Once we extracted the sediment from the profiles using the  
24  
25 284 cylinders, these were wrapped using aluminium foil still inside of the cloth. The  
26  
27 285 cylinders were labelled with their respective code and depth. After labelling,  
28  
29 286 ~200 g of the sediment was extracted from the periphery of the samples  
30  
31 287 selected for the full OSL dating. The material was placed in small bags and  
32  
33 288 labelled according to their assigned codes.  
34  
35  
36  
37  
38  
39  
40

#### 41 PPSL analysis

42  
43 291  
44  
45  
46 292 To measure the luminescence signals coming from the samples extracted at  
47  
48 293 the UGRB we used the PPSL unit build at the Scottish Universities  
49  
50 294 Environmental Research Centre (SUERC), UK. The analyses were performed  
51  
52 295 at the Irradiation Unit of the Research Institute of Nuclear Sciences of the  
53  
54 296 *Universidad Nacional Autónoma de México*, Mexico. The Infra-Red Stimulated  
55  
56 297 Luminescence (IRSL) is the optical stimulation available at the PPSL reader  
57  
58  
59  
60

298 and that was used to stimulate the samples. The PPSL unit has a  
299 photomultiplier with U-340 detection filters to measure the Anti-Stokes  
300 luminescence received from the stimulated samples that generates photons  
301 detected and quantified with high sensitivity using a digital lock-in photon  
302 counting method. A total of 130 samples were analysed with the PPSL from  
303 the nine profiles selected in fieldwork (i.e. USU1, USU2, USU3, USU13-1,  
304 USU13-2, GRIJ-PA1, GRIJ-PA2, GRIJ-PB1 and GRIJ-PB2).

305  
306 The material analysed contained ~5 grams of polymineral and polygrain-size  
307 sediments. In laboratory, the samples were processed under safe red light to  
308 avoid any bleaching of grains at their preparation and subsequent reading.  
309 The samples were not chemically treated and were not sieved before being  
310 placed in petri-dishes for their stimulation in the PPSL unit. We followed the  
311 procedures described by Sanderson and Murphy, (2010) and Muñoz-Salinas  
312 et al., (2011; 2014).

313  
314 **Full OSL dating**

315  
316 The full OSL dating method consists of obtaining equivalent doses and dose  
317 rates for calculating the age of the deposits (Aitken, 1995; 1998). A total of 8  
318 samples were selected for applying the full OSL dating method. These are  
319 located at profiles USU2, USU13-1, USU13-2 and GRIJ-PA1. The samples  
320 were sent to the SUERC laboratory in UK.

321

1  
2  
3 322 In the laboratory, all samples were handled under safelight conditions.  
4  
5 323 Samples from the Grijalva River (profile GRIJ-PA1) were labelled as SUTL  
6  
7 324 numbers 2508 and 2509. Samples from the Usumacinta River were labelled  
8  
9 325 depending on the profile as: (1) USU2 with the codes of SUTL numbers 2511,  
10  
11 326 2512 and 2513, (2) USU13-1, with the numbers of 2580, and 2581 and (3)  
12  
13 327 USU13-2, with the numbers of 2583, 2584, and 2585.  
14  
15  
16 328

17  
18 329 The SAR protocol was used in order to calculate the equivalent doses of  
19  
20 330 samples since this protocol allows correcting changes in sensitivity in the  
21  
22 331 luminescence signals (Murray and Roberts, 1998; Murray and Wintle, 2000;  
23  
24 332 Kinnaird et al., 2012; 2014). To apply the SAR protocol, 16 aliquots were  
25  
26 333 initially prepared for each sample. However, some aliquots did not yield  
27  
28 334 equivalent doses and for some samples, more aliquots were prepared. Thus,  
29  
30 335 the number of aliquots used for the calculation for the full OSL dating is  
31  
32 336 different from sixteen (see Table 1). Each aliquot was placed in a stainless  
33  
34 337 steel disc of ~10 mm mounted with ~200-300 grains of quartz in the fraction of  
35  
36 338 125-250  $\mu$  m. For grain size selection, wet sieve between 125 and 250  $\mu$  m  
37  
38 339 was done. In order to dissolve less chemically resistant minerals and to etch  
39  
40 340 the outer part of the grains and to obtain just grains of quartz, the samples  
41  
42 341 were leached with 1M 40% HF for 40 minutes and 1M 40% CIH for 10  
43  
44 342 minutes. The remaining grains were centrifuged in sodium polytungstate  
45  
46 343 solution to separate the quartz fraction from heavy metal grains. The selected  
47  
48 344 quartz fraction was then subjected to further leaching with HF and HCl (1M  
49  
50 345 40% HF for 40 minutes, followed by 1M HCl for 10 minutes). All samples were  
51  
52 346 dried at 50 °C and transferred to Eppendorf tubes.  
53  
54  
55  
56  
57  
58  
59  
60

347

348 The aliquots were placed in the carousel of an automated Risø TL/OSL DA-  
349 15 that is equipped with: (1) diodes in the blue stimulation emitting around 470  
350 nm and diodes in the infrared (laser) stimulation emitting around 830 nm for  
351 optical stimulation, (2) U-340 detection filters to detect in the region 270-380  
352 nm and (3) an irradiation  $\beta$ -source Sr90/Y90 (Bøtter-Jensen et al., 2000).

353 Regenerative dose responses curves were obtained using the natural readout  
354 and followed by cycles of readout after several irradiations of 1, 5, 10 and 20  
355 Gy, with a test dose of 2 Gy. For equivalent dose determination, data from  
356 SAR measurements were analysed using the Risø TL/OSL Viewer programme  
357 to export integrated summary files that were analysed in MS Excel® and  
358 SigmaPlot®. Composite dose response curves and radial plots were  
359 constructed from selected discs. The radial plots indicated the mean, median,  
360 robust mean, logged and non-logged central age modelled mean of Galbraith  
361 et al., (1999). The robust mean was calculated by an MS Excel® add-in  
362 “robust statistics” available from the Chemistry Society of London, which  
363 calculates a robust mean using Huber’s estimate 2.

364

365 Dose rates of irradiation were calculated using bulk quantities of the material  
366 extracted from the surrounding perimeter of the tube samples and it was  
367 measured using a high-resolution gamma spectrometer. In order to do the  
368 dose rate analysis, the material was placed in an oven to dry to constant  
369 weight. Approximately 100 g of the dried material from each sample was used  
370 for the high-resolution gamma spectrometry measurement. Gamma ray  
371 spectra were recorded over the 30 keV to 3 MeV range from each sample,



interleaved with background measurements and measurements from SUERC Shap Granite standard in the same geometries. Counting times of 80 ks per sample were used. The spectra was analysed to determine count rates from the major line emissions from  $^{40}\text{K}$  (1461 keV), and from selected nuclides in the U decay series ( $^{234}\text{Th}$ ,  $^{226}\text{Ra}$ ,  $^{235}\text{U}$ ,  $^{214}\text{Pb}$ ,  $^{214}\text{Bi}$  and  $^{210}\text{Pb}$ ) and thorium decay series ( $^{228}\text{Ac}$ ,  $^{212}\text{Pb}$ ,  $^{208}\text{Tl}$ ) including their statistical counting uncertainties. Net rates and activity concentrations for each of these nuclides were determined relative to Shap Granite by weighted combination of the individual lines for each nuclide. The internal consistency of nuclide specific estimates for uranium and thorium decay series nuclides was assessed relative to measurement precision, and weighted combinations used to estimate mean activity concentrations ( $\text{Bq kg}^{-1}$ ) and elemental concentrations (% K and ppm U, Th) for the parent activity. These data were used to determine infinite matrix dose rates for alpha, beta and gamma radiation (Kinnaird et al., 2012; 2014). To calculate the final dose rates, the cosmic dose rate contribution was calculated based in Prescott and Hutton (1994).

388

### 389 Profiling OSL dating

390

The profiling OSL dating method consists of obtaining apparent ages by using equivalent doses calculated for the sample and dose rates obtained not for the sample but for the adjacent full OSL dating sample extracted from the same sampling profile. Using the profiling OSL dating method it is assumed that the

395 sediment studied in the profile is similar in the radionuclide concentration. To  
396 perform the profiling OSL dating method it is necessary to firstly know the age  
397 via the full OSL dating method (Burbidge et al., 2007; Sanderson et al., 2007;  
398 Muñoz-Salinas et al., 2014). The profiling OSL dating analysis was also done  
399 at the SUERC laboratory in UK where all samples were managed under  
400 safelight.

401

402 We extracted 16 samples for the profiling OSL dating method in the same four  
403 profiles selected for the full OSL dating. In laboratory, these profiling samples  
404 were named with the code of the closest full OSL dating sample and followed  
405 by a letter. For the Grijalva River (profile GRIJ-PA1) samples were labelled as  
406 SUTL 2510A, 2510B and 2510C. Samples from the Usumacinta River were  
407 labelled depending on the profile as: (1) USU2 with the codes of SUTL 2514A,  
408 2514B and 2514C, (2) USU13-1, with the codes SUTL 2581A, 2582B, 2582C,  
409 and 2582D and (3) USU13-2, with the numbers and letters 2586A, 2586B,  
410 2586C, 2586D, 2586E and 2586F.

411

412 To calculate equivalent doses in the profiling OSL dating samples, two aliquots  
413 were prepared following the procedures described for the full OSL dating  
414 method. The SAR protocol was used to obtain luminescence signals, using the  
415 Risø TL/OSL. The total dose rate used for the profiling was estimated by  
416 extrapolating the dose rate trend through the closer full OSL dating locations  
417 or by taken directly the dose rate of the closest full OSL dating sample.

418

## 419 Results

420

### 421 PPSL system results

422

423 The luminescence values obtained from the nine sampling profiles of the  
424 UGRB do not exhibit a steady decrease of luminescence values from the  
425 bottom to the top as expected in the ideal situations for OSL dating when there  
426 is succession of well-reset deposits (Fig. 6). Instead, in all of the nine profiles  
427 the luminescence values show a random pattern resembling the succession of  
428 poorly reset deposits that deviate from the ideal situation for OSL dating (see  
429 for comparison the luminescence signals obtained for the sequence of lahar  
430 deposits at Popocatepetl volcano; Fig. 1B).

431

### 432 Full OSL dating results

433

434 The two samples located in the Grijalva River at profile GRIJ-PA1 (SUTL 2508  
435 and 2509) show a variable equivalent dose distribution (Fig. 7). As a result, the  
436 ages obtained for these two samples have uncertainties of hundreds of years,  
437 as it can be observed in the resulting calendar years of  $1120 \pm 350$  AD  
438 (SUTL2508) and  $550 \pm 270$  AD (SUTL2509) (Table 2). There is progression of  
439 the two ages with depth since sample SUTL2508 at 0.49 m depth is younger  
440 ( $1120 \pm 350$  AD) than sample SUTL2509 at 1.36 m depth ( $550 \pm 270$  AD).

441

1  
2  
3 442 The eight samples located in the Usumacinta River, three at profile USU2  
4  
5 443 (SUTL2511, 2512 and 2513), two at profile USU13-1 (SUTL2580 and 2581)  
6  
7 444 and three at profile USU13-2 (SUTL2582, 2583 and 2584) do not have a high  
8  
9 445 scatter of palaeodoses compared with those samples observed for the Grijalva  
10  
11 446 River (Fig. 8). The resulting ages in the Usumacinta River have uncertainties  
12  
13 447 of decades (Table 2). In profiles USU2 and USU13-1, the resulting calendar  
14  
15 448 years exhibit older ages at deeper parts of the profile, as expected. In profile  
16  
17 449 USU13-2 the increase of age with depth occurs for samples SUTL2583 and  
18  
19 450 2584 but not for sample SUTL2585, what is located in the bottom of the  
20  
21 451 profile.  
22  
23  
24  
25  
26

27 453 Profiling OSL dating results

28  
29  
30  
31 454 The equivalent doses obtained for the two aliquots for each profiling sample  
32  
33 455 are presented in Table 3. From the profiling data (Table 3) it can be observed  
34  
35 456 that in ten of the sixteen samples the difference between the two aliquots is  
36  
37 457 greater than 1 Gy. The mean value of the equivalent doses obtained for  
38  
39 458 aliquot 1 and 2 was used in the apparent age calculation presented in Table 2.  
40  
41  
42

43 459

44  
45  
46 460 In profile GRIJ-PA1 the profiling ages are older with depth as was expected  
47  
48 461 from our initial hypothesis. However if both the profiling and full OSL dating  
49  
50 462 samples are considered for interpreting the whole profile, it can be observed  
51  
52 463 that there is not a clear trend between the age and depth. The uncertainties of  
53  
54 464 ages are of hundreds of years as was also the case for the full OSL dating  
55  
56 465 ages for the Grijalva River.  
57  
58  
59  
60

466

467 In profile USU2 the profiling and full OSL ages show a scaling between the  
468 age and depth with exception of the sample located at the bottom of the profile  
469 (i.e., between 1.34 and 1.50 m depth). Sample SUTL2514C is apparently  
470 younger (AD 1490) than SUTL2513 (AD 1620). However the uncertainty of the  
471 age calculated for the profiling sample SUTL2514C is higher than for the full  
472 OSL sample SUTL2513. Apart from SUTL2514C that contains an uncertainty  
473 of more than a century, the rest of the ages in profile USU2 are within the  
474 order of decades. The profiling sample 2514B (AD 1620) was taken at the  
475 same depth of the full OSL dating sample SUTL2512 (AD 1670) however they  
476 have a difference of 50 years and the same uncertainty in their age.

477

478 In profile USU13-1 the profiling ages are older with depth as expected since  
479 the SUTL2582A at 0.2 m depth is, according to the results, older than  
480 SUTL2582B at 0.6 m depth. However, the ages including profiling and full OSL  
481 ages only have a good progression from 0.6 m to 1.4 m of depth. Most of the  
482 samples contain uncertainties of several decades, except for the two profiling  
483 samples at the top and the bottom that contain uncertainties of hundreds of  
484 years.

485

486 In profile USU13-2 the profiling and full OSL ages correlate with depth only in  
487 the first 1.25 m (see values in Table 2 and Fig. 5). Below the 1.5 m depth,  
488 ages have a random pattern. In profile USU13-2 there are some samples that

489 contain high uncertainties, such as sample SUTL2586D that has an  
490 uncertainty in the order of thousands of years.

491

492 **Discussion**

493

494 All the results obtained by the three different OSL methods indicate that the  
495 young fluvial sediments located in the floodplains of the Usumancinta and  
496 Grijalva rivers are incompletely reset. Such behaviour contrasts with our initial  
497 hypothesis. The PPSL signals of the nine profiles revealed an increase and  
498 decrease of luminescence at different depths of each profile (Fig. 6). Such a  
499 random luminescence trend versus depth was observed in poorly reset  
500 sediment profiles, as contrary to the progressive increase of luminescence  
501 from top to bottom in well-reset sediments (Fig. 1A).

502

503 The radial plots including the distribution of equivalent doses calculated for the  
504 aliquots prepared for the full OSL dating samples reveal that there is great  
505 variability of our data (Figs. 7 and 8). Also, the equivalent doses for the two  
506 aliquots prepared for most of the profiling samples show a large variability  
507 (Table 2).

508

509 The uncertainties calculated for the profiling and full OSL samples based in  
510 the equivalent doses and dose rates highlight the large uncertainty in the OSL  
511 ages which range from decades to hundreds of years and one of them with a  
512 thousands of years (Table 2).

1  
2  
3 513  
4

5 514 Advantages and limitations in the three OSL methods  
6  
7

8 515  
9

10 516 The PPSL analysis can be used as a proxy to the grade of resetting of  
11  
12 517 sediment in a profile composed by a succession of deposits. Muñoz-Salinas et  
13  
14 518 al., (2011; 2012; 2014) and Portenga and Bishop (2015) showed the  
15  
16 519 usefulness in using the PPSL analysis to identify different depositional  
17  
18 520 processes and sediment transport rates of grains in fluvial environments. We  
19  
20 521 cited two types of scenarios of luminescence patterns. In the first one we  
21  
22 522 presented the case of the deposits consisting of well-reset fluvial sediment of  
23  
24 523 Lachlan River in Australia (Fig. 1A) and in the second one we presented the  
25  
26 524 example of a poorly reset fluvial sediment in the Popocatepetl volcano (Fig.  
27  
28 525 1B). In the first case, the fluvial sediments were transported in dilute flows and  
29  
30 526 in the second one, the fluvial sediments were mobilized in turbid and/or hyper-  
31  
32 527 concentrated flows. The luminescence patterns observed in the nine profiles of  
33  
34 528 the UGRB resemble the luminescence pattern observed in the lahar deposits  
35  
36 529 of the Popocatepetl volcano. We postulate that hyper-concentrated transport  
37  
38 530 may be a plausible explanation for the random pattern of luminescence  
39  
40 531 detected on the deposits that compose the young fluvial sediment at the  
41  
42 532 Usumacinta and Grijalva rivers. We propose that using the PPSL analysis is a  
43  
44 533 reliable tool for detecting luminescence patterns in sediments that may be  
45  
46 534 helpful to infer the flow conditions in which the sediment was transported. An  
47  
48 535 increase in luminescence from the top of the deposit to the bottom would  
49  
50 536 indicate a condition where the sediment was transported by flows that allowed  
51  
52 537 the exposure of grains to sunlight. This situation usually occurs when grains  
53  
54  
55  
56  
57  
58  
59  
60

538 travel for large distances and/or grains are mobilized in clear water. In  
539 contrast, a random pattern in the luminescence with depth can be indicative of  
540 sediment mobilized in hyper-concentrated flows, where the grains are not fully  
541 exposed to sunlight due to turbidity or because grains were mobilized in a  
542 short time.

543

544 The application of the full OSL dating method is currently one of the more  
545 commonly used methods in many geomorphologic studies. The dating with  
546 OSL is a powerful geochronological tool for dating fluvial deposits, which can  
547 also provide information about the grade of resetting of the grains by  
548 interpreting the radial plots of equivalent doses and by setting their respective  
549 uncertainties. In the case of the Usumacinta and Grijalva rivers, the full OSL  
550 dating revealed a large variability of the equivalent doses, as a consequence,  
551 large uncertainties were obtained for the calculated ages.

552

553 The profiling OSL method is less applied than the full OSL method, since this  
554 first technique is less precise for the calculation of ages compared to the full  
555 OSL dating. Nevertheless, the dating with OSL profiling has lower costs than  
556 the full OSL dating and can be used to identify differences in depositional rates  
557 in fluvial landscapes. Muñoz-Salinas et al., (2014) used both the full OSL  
558 method and profiling for dating several deposits located at different depths in a  
559 well-reset succession of fluvial sediments in the Lachlan River in Australia. In  
560 that study, the ages in the profiling and full OSL samples revealed a good  
561 trend of luminescence versus depth. However, in the study of the Usumacinta  
562 and Grijalva rivers, the profiling method did not provide accurate ages.



Moreover, the approach revealed inconsistencies in the age of sediment. We postulate the use of OSL profiling is suitable only in sites where deposits contain well-reset sequences along the profiles. In order to prevent unnecessary expenses for either the full OSL dating and the profiling OSL method, the analysis using PPSL is here highly recommended before dating the sediment.

#### Poorly reset deposits in the recent fluvial sediments of the UGRB

In tropical areas the cyclonic activity is intensified during the summer periods but also the rate and magnitude of the cyclonic activity change every year (Grotsky and Carton, 2003). Therefore, intense stormy events (lasting from minutes to a few days) can promote intense episodes that can trigger hyper-concentrated and turbid flows (Beach et al., 2008; Rosengaus-Moshinsky et al., 2002). These kinds of flows are able to inundate the overbanks of channels and leave deposits containing grains that are unlikely to be bleached during their transport. In our study we focused in the analysis of samples abandoned overbank. We suspect that some of the sediments were deposited by turbid and hyper-concentrated flows that took place during rapidly eroding episodes on the river basin. Moreover, in large basins like the UGRB, the source of the grains deposited in the floodplains may be transported from close areas or from far distances, thus, a mixture of grains with different travel histories and resetting grades can be composing part of the deposits of the floodplain.

588 To explore the source of grains we have plotted the maximum PPSL  
589 luminescence values in the Usumacinta and Grijalva profiles versus the  
590 distance from the basin divide (Fig. 9). In Figure 9 it can be observed how  
591 luminescence values decrease within distance from the divide as grains are  
592 exposed to sunlight for longer periods of time. For the case of the Lachlan  
593 River (Muñoz-Salinas et al., 2014), the maximum luminescence values  
594 decrease with distance to the divide indicating that the main source of the  
595 material deposited by the river came from the mountain area (see in Fig. 9 the  
596 of  $R^2 = 0.56$  of IR luminescence signals versus distance from divide).  
597 However, in the case of the Usumacinta and the Grijalva rivers the correlation  
598 is weak, suggesting that the sediment source may not be from far away (see in  
599 Fig. 9 that the correlation for the Grijalva River is of  $R=0.48$  and for the  
600 Usumacinta River of  $R=0.14$ ). We suggest that sediment at the floodplains of  
601 the Usumacinta and Grijalva rivers is partially connected in the river system  
602 and by hence, most of the sediment is stored at the floodplains of the rivers  
603 during some time and it can only be mobilized (and reconnected) during  
604 extreme flood events; as it is described by Hooke (2003). Therefore, grains at  
605 the floodplains of the Usumacinta and Grijalva rivers contain mixed reset  
606 histories that are highly likely responsible for the variability observed in the  
607 equivalent doses in the profiling and full OSL dating samples here.

608

609 The dose rates are also related to the luminescence signals as it was detected  
610 from the random values observed in the dose rates of the Grijalva and  
611 Usumacinta profiles (Table 2). The changes in the dose rates are conditioned  
612 by the amount of radionuclides contained in each deposit. In a large basin like

the UGRB in which the sediment source may be produced from different types of lithology (see Fig. 3B) and in which sediment can be eroded from different places of the riverbasin, the concentrations of radionuclides can have different concentration depending on the lithology.

Finally, even though the sedimentological processes described in this study may increase the errors and uncertainties in the ages calculated by the full OSL and profiling dating methods, most of the ages indicate that the sedimentation in the main channel of the Usumacinta and Grijalva rivers in the floodplain started during the Classic period of the Maya Civilization. Therefore the sedimentation observed in the main channels of the UGRB is less than two thousand years (see Table 2).

We minimized the impact of dams in the reset grade of the sediments studied here because: (1) the dams are only constructed in the Grijalva River and not in the Usumacinta River and we have either poorly reset sediment in the Grijalva and in the Usumacinta rivers and (2) the first dam was built in 1968 and the ages obtained for the samples are older than that age.

## Conclusions

The three methods used in this research to study young fluvial sediments at the floodplains of the Usumacinta and Grijalva rivers strongly indicate that most of the grains deposited at the floodplain of the UGRB are partially bleached during their transport. The PPSL analysis allowed the detection of

luminescence patterns of incomplete reset deposits that may have been resulted from the transport of these by turbid and hyper-concentrated flows. The profiling and full OSL dating indicate that the sediment contains large variability in their equivalent doses resulting in large uncertainties on the calculated ages. Such variability explains errors from several decades to thousands in our samples of the Holocene. We propose that the use of the PPSL analysis is a powerful tool to detect poorly reset sequences of deposits. Such approach is useful in order to reduce the costs of OSL dating, especially in the profiling with OSL. We also conclude that the possible causes of the incomplete bleaching of the young sediments of the UGRB found at the floodplains is probably related to the cyclonic activity controlling the discharge of rivers in the basin which may be enhanced with high-magnitude cyclones producing turbid and hyper-concentrated flows.

*Acknowledgments*-This study was funded by two DGPA-PAPIIT grants (numbers IB100812 and IA102615) from the Universidad Nacional Autónoma de México. The authors thank to the editor, associate editors and anonymous reviewers involved in the revision of this manuscript for their thoughtful critiques and appropriate suggestions that notably improved the first version of the manuscript.

**REFERENCES**

Aitken, M. J. 1995. Thermoluminescence dating: past progress and future trends. *Nuclear Tracks* **10**: 3–6.

- 663 Aitken, M. J. 1998. *An Introduction to Optical Dating. The Dating of Quaternary*  
664 *Sediments by the Use of Photon Stimulated Luminescence*. New York: Oxford  
665 University Press.
- 666 Beach, T. Luzzadder-Beach, S., Dunning, N., & Cook, D. 2008. Human and  
667 natural impacts on fluvial and karst depressions of the Maya Lowlands.  
668 *Geomorphology* **101**: 308-331.
- 669 Benjamin, T. 1981. El trabajo en las monterías de Chiapas y Tabasco, 1870-  
670 1946. *Historia Mexicana* **30**: 506-529.
- 671 Benke, A.C. 2009. Streams and Rivers of North America: Western, Northern  
672 and Mexican Basins. In Linkens G. (Ed.), *Encyclopedia of Inland Waters*.  
673 Oxford, UK, Elsevier.
- 674 Bøtter-Jensen, L., Bulur, E., Duller, G.A.T, Murray, A.S., 2000. Advances in  
675 luminescence instrument systems. *Radiation Measurements* **32**: 523-528.
- 676 Brook, G.A., Srivastava, P., Marais, E., 2006. Characteristics and OSL  
677 minimum ages of relict fluvial deposits near Sossus Vlei, Tsauchab River,  
678 Namibia, and a regional climate record for the last 30 ka. *Journal of*  
679 *Quaternary Science* **21**: 347-362.
- 680 Burbidge CI, Sanderson DCW, Housley RA, & Jones PA. 2007. Survey of  
681 palaeolithic sites by luminescence profiling, a case study from Eastern Europe.  
682 *Quaternary Geochronology* **2**: 296-302.
- 683 Cros, P., Michaud, F., Fourcade, E., & Fleury, J-J. 1998. Sedimentological  
684 evolution of the Cretaceous carbonate platform of Chiapas (Mexico). *Journal*  
685 *of South American Earth Sciences* **11**: 311-332.
- 686 Day, J.W., Yañez-Arancibia, A., Mitsch, W.J., Lara-Dominguez, A.L., Day, J.N.,

1  
2  
3  
4  
5  
6  
7  
8  
9  
10  
11  
12  
13  
14  
15  
16  
17  
18  
19  
20  
21  
22  
23  
24  
25  
26  
27  
28  
29  
30  
31  
32  
33  
34  
35  
36  
37  
38  
39  
40  
41  
42  
43  
44  
45  
46  
47  
48  
49  
50  
51  
52  
53  
54  
55  
56  
57  
58  
59  
60

687 Duller, G.A., 2004. Luminescence dating of Quaternary sediments: recent  
688 advances. *Journal of Quaternary Science* **19**: 183-192.

689 Duller, G.A., 2008. Single-grain optical dating of Quaternary sediments: why  
690 aliquot size matters in luminescence dating. *Boreas* **37**: 589-612

691 Galbraith, R.F., Roberts, R.G., Laslett, G.M., Yoshida, H., Olley, J.M., 1999.  
692 Optical dating of single and multiple grains of quartz from Jinmium rock  
693 shelter, northern Australia: Part I, Experimental design and statistical models.  
694 *Archaeometry* **41**: 339-364.

695 Grodsky, S.A., & Carton, J.A. 2003. The intertropical convergence zone in the  
696 South Atlantic and the equatorial cold tongue. *Journal of Climate* **16**: 2052-  
697 2065.

698 Hirth, K., Cyphers, A., Cobean, R., De León, J., & Gascock, M.D. 2013. Early  
699 Olmec obsidian trade and economic organization at San Lorenzo. *Journal of*  
700 *Archaeological Science* **40**: 2784-2798.

701 Hooke, J., 2003. Coarse sediment connectivity in river channel systems: a  
702 conceptual framework and methodology. *Geomorphology* **56**: 79-94.

703 Hudson, P., Hendrickson, D.A., Benke, A.C., Varela-Romero, A., Rodiles-  
704 Hernández, R. Minckley, W.L., 2005. *Rivers of Mexico*. In: Benke, A.C. and  
705 Cushing, C.E. (eds.), *Rivers of North America*. Elsevier Academic Press, San  
706 Diego, CA, USA.

707 Kinnaird, T.K., Sanderson, D., & Muñoz-Salinas, E. 2011a. OSL dating of  
708 sediment from the Grabben Gullen Creek, upper Lachlan River Catchment, SE  
709 Australia. Technical Report. Scottish Universities Environmental Research

- 710 Centre, UK.
- 711 Kinnaird, T.K., Sanderson, D., & Muñoz-Salinas, E. 2011b. OSL dating of  
712 fluvioglacial and post-glacial debris flow deposits in the Gredos mountain  
713 range, Central Spain. Technical Report. Scottish Universities Environmental  
714 Research Centre, UK.
- 715 Kinnaird, T.K., Sanderson, D., & Muñoz-Salinas, E. 2012. *Using Optically*  
716 *Stimulated Luminescence to Unravel Sedimentary Processes of the*  
717 *Usumacinta and Grijalva Rivers (SE Mexico)*. Technical Report. Scottish  
718 Universities Environmental Research Centre, UK.
- 719 Kinnaird, T.K., Muñoz-Salinas, E., Sanderson, D., Castillo, M., Cruz-Zaragoza,  
720 E. 2014. *OSL characterization of two fluvial sequences of the River*  
721 *Usumacinta in its middle catchment (SE Mexico)*. Technical Report. Scottish  
722 Universities Environmental Research Centre, UK.
- 723 Kunk, A., Pflanz, D., Weniger, T., Urban, B., Kruger, F., & Chen, Y-G. 2013.  
724 Optically Stimulated Luminescence Dating of Young Fluvial Deposits of the  
725 Middle Elbe River Flood Plains using different age models. *Geochronometria*  
726 **41**: 36-56.
- 727 Marshall, J.S. 2007. Geomorphology and Physiographic Provinces of Central  
728 America. In Bundschuh, J. & Alvarado G. (Eds.), *Central America: Geology,*  
729 *Resources , and Hazards*. London, UK, Taylor and Francis.
- 730 Morán-Zenteno, D.J., Tolson, G., Martínez-Serrano, R.G., Martiny, B., Schaaf,  
731 P., Silva-Romo, G., Macías-Romo, C., Alba-Aldave, L., Hernández-Bernal,  
732 M.S., & Solís-Pichardo, G.N. 1999. Tertiary arc-magmatism of the Sierra

733 Madre del Sur, Mexico, and its transition to the volcanic activity of the Trans-  
734 Mexican Volcanic Belt. *Journal of South American Earth Sciences* **12**: 513-  
735 535.

736 Muñoz-Salinas, E., Bishop, P., Sanderson, D., & Zamorano, J-J. 2011.  
737 Interpreting luminescence data from a portable OSL reader: three case studies  
738 in fluvial settings. *Earth Surface Processes and Landforms* **36**: 651-660.

739 Muñoz-Salinas, E., Bishop, P., Sanderson, D., & Zamorano, J-J. 2012.  
740 Sedimentological processes in Lahars: insights from Optically Stimulated  
741 Luminescence analysis. *Geomorphology* **136**: 106-113.

742 Muñoz-Salinas, E., & Castillo, M., 2013. Sediment and water discharge  
743 assessment on Santiago and Pánuco Rivers (Central Mexico): The importance  
744 of topographic and climatic factors. *Geografiska Annalers: Series A, Physical*  
745 *Geography* **95**: 171-183.

746 Muñoz-Salinas, E., Bishop, P., Sanderson, D., & Kinnaird, T. 2014. Using OSL  
747 to assess hypotheses related to the impacts of land use change with the early  
748 nineteenth century arrival of Europeans in south-eastern Australia: An  
749 exploratory case study from Grabben Gullen Creek, New South Wales. *Earth*  
750 *Surface Processes and Landforms* (published online).

751 Muñoz-Salinas, E., & Castillo, M., 2015. Streamflow and sediment load  
752 assessment from 1950 to 2006 in the Usumacinta and Grijalva rivers  
753 (Southern Mexico) and the influence of ENSO. *Catena* **127**: 270-278.

754 Murray, A.,S & Roberts, R.G., 1998. Measurement of the equivalent dose in  
755 quartz using a regenerative-dose single aliquot protocol. *Radiation*  
756 *Measurements* **29**: 503-515.



- 1  
2  
3 757 Murray, A.S., & Wintle, A.G. 2000. Luminescence dating of quartz using and  
4  
5 758 improved single-aliquot regenerative-dose protocol. *Radiation Measurements*  
6  
7 759 **32**: 57-73.  
8  
9  
10 760 Lomax, J., Hilgers, A., Twidale, C.R., Bourne, J.A., & Radtke, U. 2007.  
11  
12 761 Treatment of broad palaeodose distributions in OSL dating of dune sand from  
13  
14 762 the western Murray Basin, South Australia. *Quaternary Geochronology* **2**: 51-  
15  
16 763 56.  
17  
18 764 Ochoa-Gaona, S., & González-Espinosa, M. 2000. Land use and deforestation  
19  
20 765 in the highlands of Chiapas, Mexico. *Applied Geography* **20**: 17-42.  
21  
22  
23 766 Portenga, E., Bishop, P., 2015. Confirming geomorphological interpretations  
24  
25 767 based on portable OSL reader data. *Earth Surface Processes and Landforms*.  
26  
27 768 Doi. 10.1002/esp.3834  
28  
29  
30 769 Prescott, J.R., Hutton, J.T., 1994. Cosmic ray contributions to dose rates for  
31  
32 770 luminescence and ESR dating: large depths and long-termtime variations.  
33  
34 771 *Radiation Measurements* **23**: 497-500.  
35  
36 772 Ramírez-Marcial, N., González-Espinosa, M., & Williams-Linera, G. 2001.  
37  
38 773 Anthropogenic disturbance and tree diversity in Montane Rain Forests in  
39  
40 774 Chiapas, Mexico. *Forest Ecology and Management* **154**: 311-326.  
41  
42  
43 775 Reyes, E., Day, J.W., Lara-Dominguez, A.L., Sanchez-Gil, P., Zarate-Lomelí,  
44  
45 776 D., & Yáñez-Arancibia, A. 2004. Assessing coastal management plans using  
46  
47 777 watershed models for the Mississippi delta, USA, and the Usumacinta-Grijalva  
48  
49 778 delta, Mexico. *Ocean & Coastal Management* **47**: 693-708.  
50  
51  
52 779 Rosengaus-Moshinsky, M., Jimenez Espinosa, M., & Vazquez Conde, M.T.  
53  
54 780 2002. *Atlas climatológico de ciclones en México*. Mexico City, Mexico: Centro  
55  
56 781 Nacional de Prevención de Desastres, CENARED.  
57  
58  
59  
60

1  
2  
3 782 Sanderson DCW, Bishop P, Stark H, Alexander S, & Penny D. 2007.  
4  
5 783 Luminescence dating of canal sediments from Angkor Borei, Mekong Delta,  
6  
7 784 Southern Cambodia. *Quaternary Geochronology* **2**: 322-329.  
8  
9  
10 785 Sanderson, D.C.W., & Murphy, S. 2010. Using simple portable OSL  
11  
12 786 measurements and laboratory characterisation to help understand complex  
13  
14 787 and heterogeneous sediment sequences for luminescence dating. *Quaternary*  
15  
16 788 *Geochronology* **5**: 1–7.  
17  
18  
19 789 Singarayer, J.S., Bailey, R.M., Ward, S., & Stokes, S., 2005. Assessing the  
20  
21 790 completeness of optical resetting of quartz OSL in the natural environment.  
22  
23 791 *Radiation Measurement* **40**: 13-25.  
24  
25  
26  
27 792 Stang, D.M., Rhodes, E.J., & Heimsath, A.M. 2012. Assessing soil mixing  
28  
29 793 processes and rates using a portable OSL-IRSL reader: Preliminary  
30  
31 794 determinations. *Quaternary Geochronology* **10**: 314-319.  
32  
33  
34 795 Weibel, L. 1998. *La Sierra Madre de Chiapas*. Mexico City, Mexico, Miguel  
36  
37 796 Angel Porrua.  
38  
39 797 Zebadua, E. 1999. *Breve historia de Chiapas*. Madrid, Fondo de cultura  
40  
41 798 económica de España.  
42  
43  
44  
45  
46  
47  
48  
49  
50  
51  
52  
53  
54  
55  
56  
57  
58  
59  
60

799 **Figure captions**

800

801 **Figure 1.** A. Profile of well–reset fluvial sediments at Lachlan River (Australia)  
802 where luminescence values (IRSL) increase with depth. Note the tight  
803 correlation where  $R^2=0.98$  (modified from Muñoz-Salinas et al., 2011). B.  
804 Profile of poorly reset grains from a lahar deposit (i.e. turbid and hyper–  
805 concentrated flow) of the Popocatepetl volcano (Mexico). In this case there is  
806 a lack of correlation between the luminescence and depth. It is evident the  
807 random increase and decrease of luminescence with the depth (modified from  
808 Muñoz-Salinas et al., 2012).

809

810 **Figure 2.** Radial plots of equivalent doses. In A most of the values are within 2  
811 standard deviations (i.e. fluvial deposits at Lachlan River, Australia; modified  
812 from Kinnaird et al., 2011a). In B most of the values are above 2 standard  
813 deviations (deposit of debris flow at Gredos Valley, Spain; modified from  
814 Kinnaird et al., 2011b). Sample SUTL2356 in A provided an age of  $2.43 \pm$   
815  $0.14$  ka with low uncertainty indicating that grains were well–reset and sample  
816 SUTL2351 in B has an age of  $10.7 \pm 1.6$  ka estimated with high uncertainty  
817 and indicating that grains may have not been fully reset.

818

819 **Figure 3.** A Location of the Usumacinta and Grijalva rivers. The Grijalva River  
820 begins at the Sierra de los Cuchumatanes and flows down between the Sierra  
821 Madre de Chiapas and Altos de Chiapas incising both mountain settings. The  
822 Usumacinta Rivers also begins at the Sierra de los Cuchumatanes but flows  
823 down the northern sector of the Altos de Chiapas. These two rivers join just a

few kilometers inland. The white circles indicate the places where the profiles for OSL analysis were taken in the Coastal Plain. (B) Sketch map of the main lithological units of the UGRB.

**Figure 4.** Cartoon of a cross-section located at the main channel of the Usumacinta and Grijalva rivers at the Coastal Plain of the Gulf of Mexico. In the figure is shown a typical location in the main channel for the vertical sediment profiles selected for sampling. The sampling sites are located on the margins eroded by the river. We avoided the accumulative margins and sites containing material from slope slides and sampling profiles with evident signs of bioturbation.

**Figure 5.** The four selected profiles in which the full OSL dating method and the profiling OSL method were applied at Usumacinta River (USU3, USU13-1 and USU13-2) and at Grijalva River (GRIJ-PA1).

**Figure 6.** Luminescence signals versus depth for the nine PPSL profiles located at the floodplains of the Usumacinta and Grijalva rivers. Note that in the nine profiles the luminescence values increase and decrease at different depths in a way similar to those reported for the trend observed of the deposits of the Popocatepetl volcano (Fig. 1B).

**Figure 7.** Scatter plots of equivalent doses for the Grijalva samples (SUTL 2508 and 2509). Notice that the equivalent doses of most of the aliquots have more than 2 sigma values indicating poor reset of the grains.

849

850 **Figure 8.** Scatter plots of equivalent doses for the Usumacinta samples (SUTL  
851 2511, 2512, 2513, 2580, 2581, 2583, 2584 and 2585). Notice that the  
852 equivalent doses of most of the aliquots have more than 2 sigma values  
853 indicating poor reset of the grains except for SUTL 2512 and 2590.

854

855 **Figure 9.** Plot of maximum IR luminescence signals for each sampling profile  
856 versus distance from divide. For comparisons are included the values  
857 published for the Lachlan River by Muñoz-Salinas et al., 2014.

858

1  
2  
3  
4  
5  
6  
7  
8  
9  
10  
11  
12  
13  
14  
15  
16  
17  
18  
19  
20  
21  
22  
23  
24  
25  
26  
27  
28  
29  
30  
31  
32  
33  
34  
35  
36  
37  
38  
39  
40  
41  
42  
43  
44  
45  
46  
47  
48  
49  
50  
51  
52  
53  
54  
55  
56  
57  
58  
59  
60

859 Table 1. Number of aliquots used for full OSL dating calculations.

860

SUTL number	Number of aliquots
2508	16
2509	29
2511	15
2512	15
2513	20
2580	12
2581	16
2583	16
2584	16
2585	16

861  
862

Table 2. OSL age determinations for samples at the Grijalva and Usumacinta rivers.

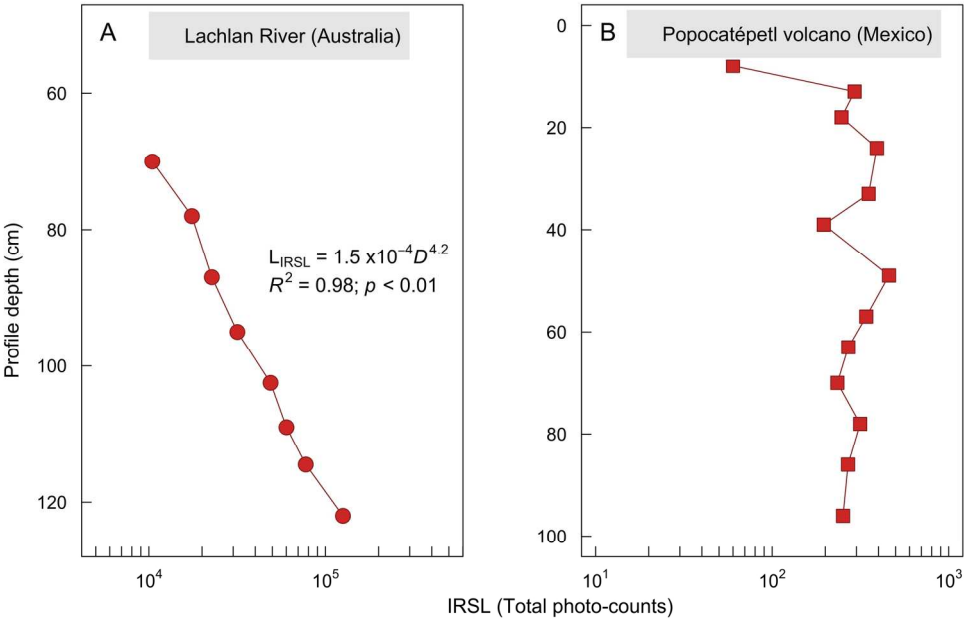
SUTL n°/ River/Profile	Depth (m)	Equivalent dose (Gy)	Dose rate (mGy a <sup>-1</sup> )	Calendar year (AD, unless stated otherwise)
<b>River Grijalva</b>				
<i>GRIJ-PA1 (2012)</i>				
2510A	0.18	6.51 ± 0.16	2.71 ± 0.16	390 ± 240
2508*	0.49	2.4 ± 0.94	2.69 ± 0.11	<b>1120 ± 350</b>
2510B	0.88	6.33 ± 1.31	2.66 ± 0.16	370 ± 510
2510C	1.18	4.96 ± 1.05	2.64 ± 0.15	130 ± 410
2509*	1.36	3.85 ± 0.68	2.63 ± 0.11	<b>550 ± 270</b>
<b>River Usumacinta</b>				
<i>USU2 (2012)</i>				
2514A	0.42	0.39 ± 0.09	4.55 ± 0.17	1920 ± 20
2511*	0.84	0.51 ± 0.10	3.65 ± 0.09	<b>1870 ± 30</b>
2514B	1.14	1.17 ± 0.07	3.00 ± 0.08	1620 ± 30
2512*	1.14	1.01 ± 0.07	3.00 ± 0.08	<b>1670 ± 30</b>
2514C	1.34	1.56 ± 0.42	2.98 ± 0.11	1490 ± 140
2513*	1.50	1.16 ± 0.08	2.95 ± 0.08	<b>1620 ± 30</b>
<i>USU13-1 (2014)</i>				
2582A	0.2	1.50 ± 0.24	2.64 ± 0.26	1450 ± 120
2580*	0.45	1.25 ± 0.11	2.86 ± 0.16	<b>1570 ± 50</b>
2582B	0.6	0.76 ± 0.03	2.64 ± 0.26	1720 ± 40
2582C	0.8	1.09 ± 0.18	2.64 ± 0.26	1600 ± 90
2581*	1.1	1.69 ± 0.07	2.93 ± 0.14	<b>1430 ± 40</b>
2582D	1.4	3.96 ± 1.05	2.64 ± 0.26	520 ± 450
<i>USU13-2 (2014)</i>				
2583*	0.25	0.77 ± 0.05	2.45 ± 0.14	<b>1700 ± 30</b>
2586A	0.5	1.06 ± 0.78	2.64 ± 0.26	1610 ± 300
2586B	0.7	1.00 ± 0.03	2.64 ± 0.26	1640 ± 50
2586C	1.0	0.24 ± 0.02	2.64 ± 0.26	1920 ± 10
2584*	1.25	1.54 ± 0.07	2.38 ± 0.14	<b>1360 ± 50</b>
2586D	1.5	14.23 ± 11.68	2.64 ± 0.26	3370 BC ± 4480
2585*	1.75	0.68 ± 0.05	2.60 ± 0.16	<b>1750 ± 30</b>
2586E	2.0	0.47 ± 0.06	2.64 ± 0.26	1840 ± 30
2586F	2.2	1.07 ± 0.47	2.64 ± 0.26	1610 ± 180

\*Age calculated using the full OSL dating method, in the rest of cases the Profiling method was used.

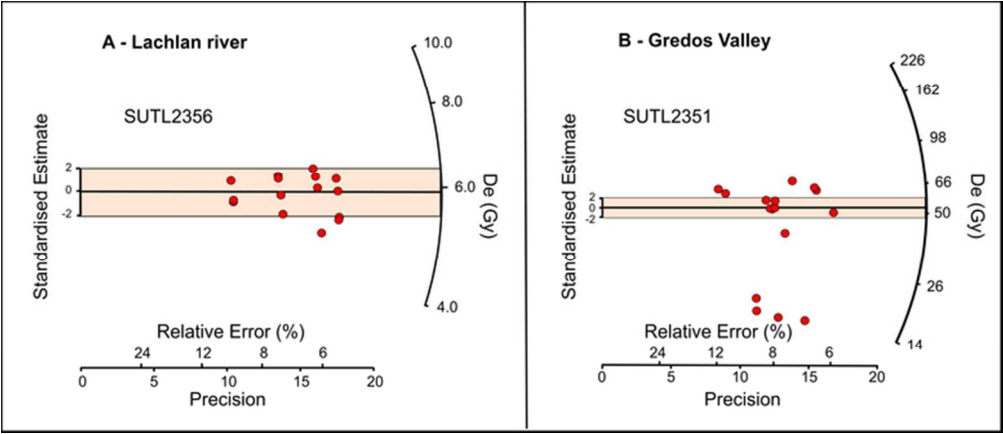
**Table 3.** Laboratory profiling results in the equivalent doses (Gy) obtained for aliquot 1 and aliquot 2. Aliquots consisted in ~200-300 grains of quartz stimulated in Blue. Variation between aliquot 1 and 2 is generally more than 1 Gy except for the six samples highlighted in bold. Note that the difference in the equivalent dose of the aliquot 1 and 2 is especially high in sample SUTL2586D.

SUTL	Depth (cm)	Equivalent dose (Gy)	
		Aliquot 1	Aliquot 2
2510A	18	5.99 ± 0.25	7.02 ± 1.00
2510B	88	7.64 ± 1.97	5.03 ± 0.62
2510C	118	3.91 ± 0.57	6.01 ± 2.99
<b>2514A</b>	<b>42</b>	<b>0.48 ± 0.06</b>	<b>0.30 ± 0.04</b>
<b>2514B</b>	<b>114</b>	<b>1.24 ± 0.12</b>	<b>1.10 ± 0.11</b>
2514C	134	1.14 ± 0.13	1.98 ± 0.13
2582A	20	1.74 ± 0.04	1.26 ± 0.07
<b>2582B</b>	<b>60</b>	<b>0.79 ± 0.04</b>	<b>0.74 ± 0.03</b>
2582C	80	0.90 ± 0.03	1.27 ± 0.05
2582D	140	5.01 ± 0.34	2.91 ± 0.21
2586A	170	0.28 ± 0.04	1.84 ± 0.12
<b>2586B</b>	<b>150</b>	<b>0.96 ± 0.12</b>	<b>1.03 ± 0.09</b>
<b>2586C</b>	<b>120</b>	<b>0.22 ± 0.03</b>	<b>0.26 ± 0.02</b>
2586D	70	25.9 ± 0.52	2.55 ± 0.16
<b>2586E</b>	<b>20</b>	<b>0.41 ± 0.05</b>	<b>0.53 ± 0.05</b>
S586F	0	1.53 ± 0.08	0.6 ± 0.05

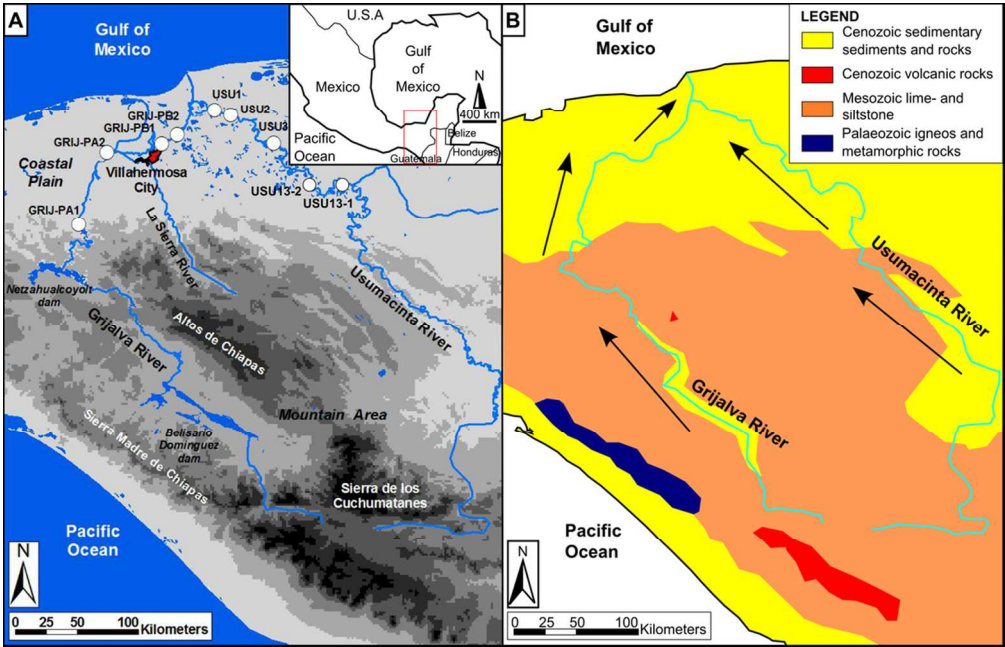




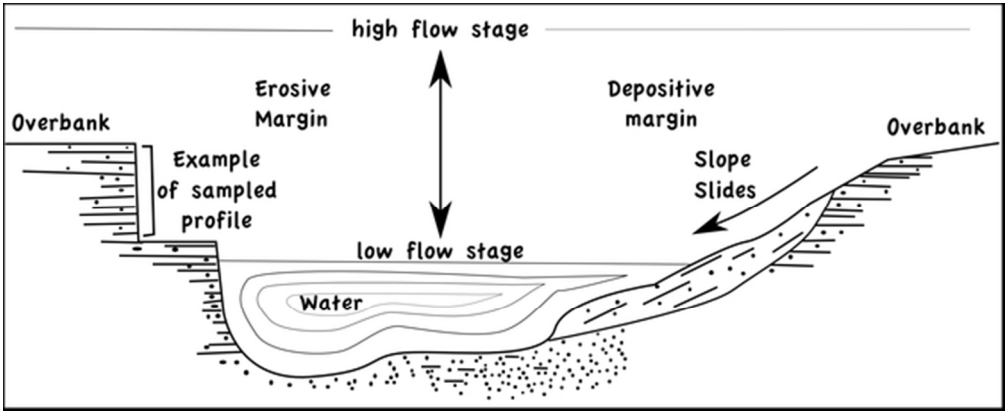
172x115mm (300 x 300 DPI)



65x28mm (300 x 300 DPI)

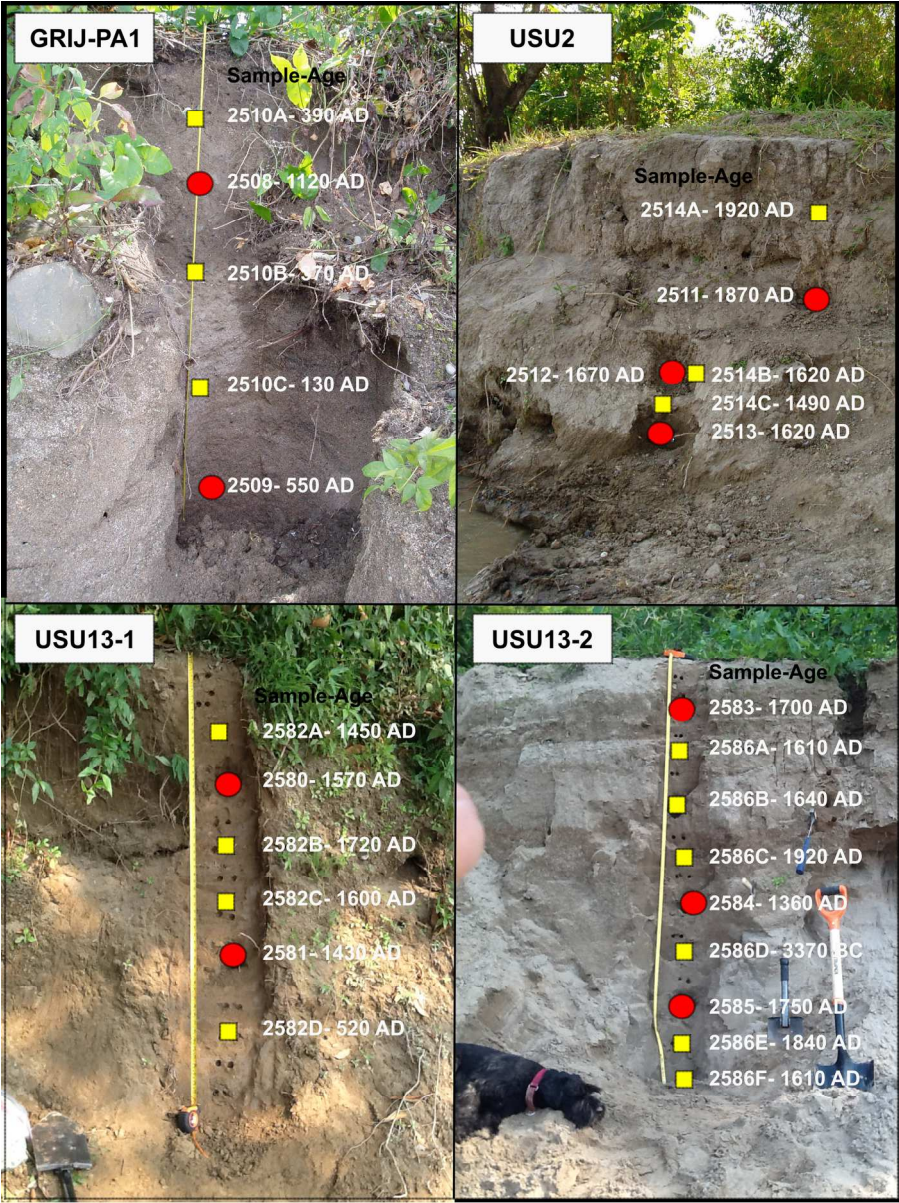


103x66mm (300 x 300 DPI)

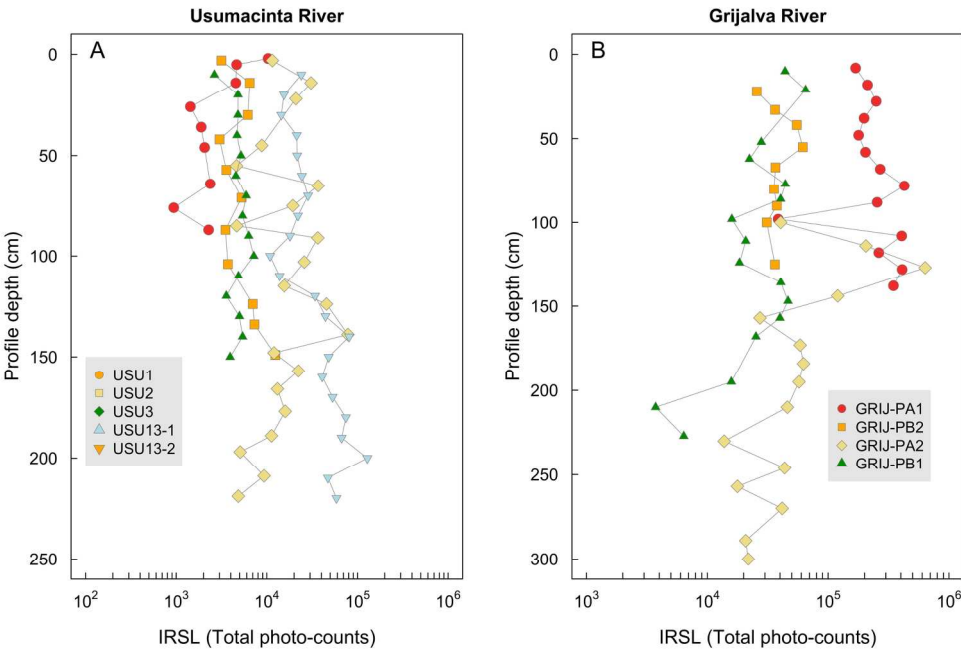


55x22mm (300 x 300 DPI)

Peer Review

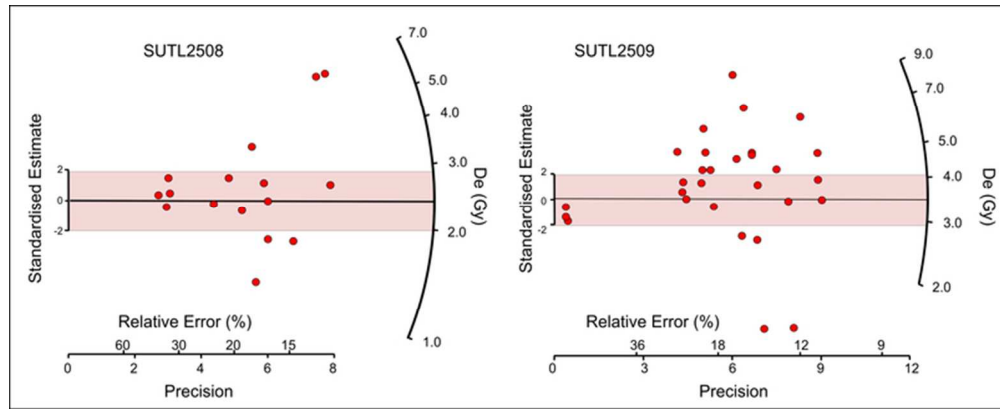


164x219mm (300 x 300 DPI)

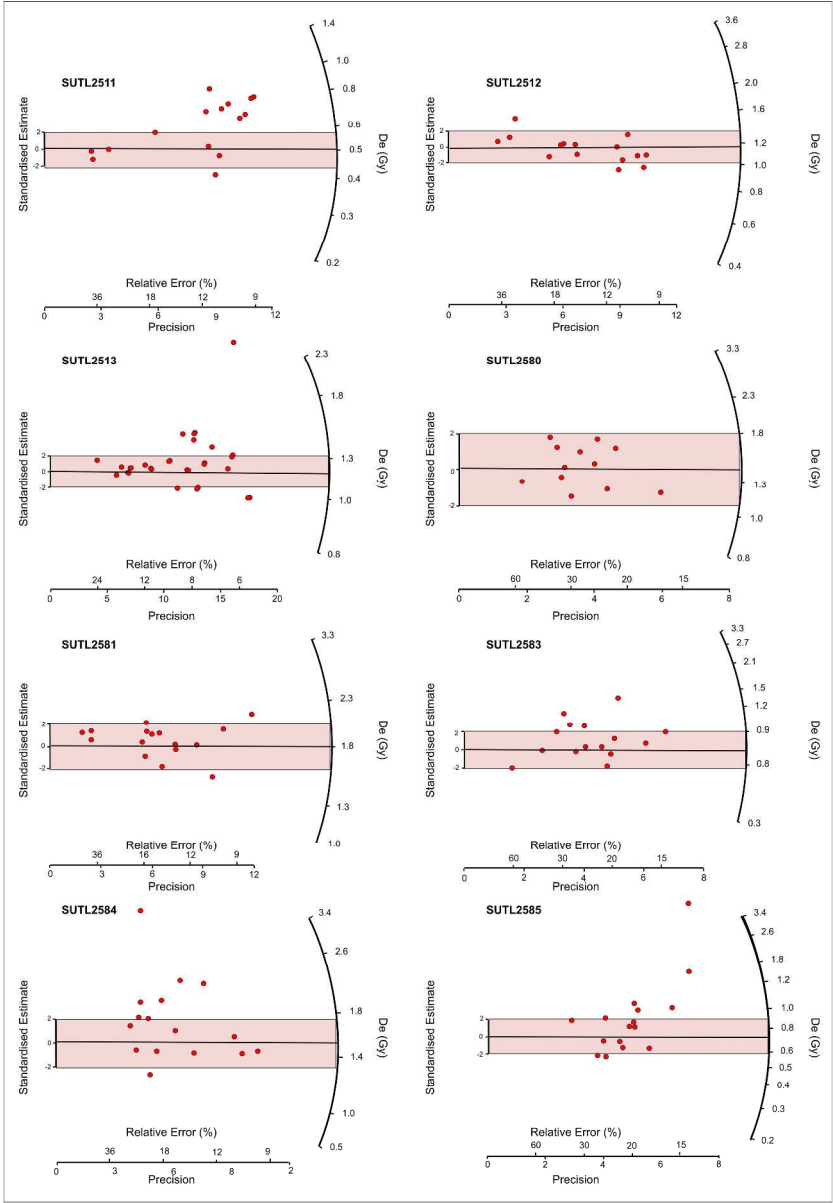


182x119mm (300 x 300 DPI)



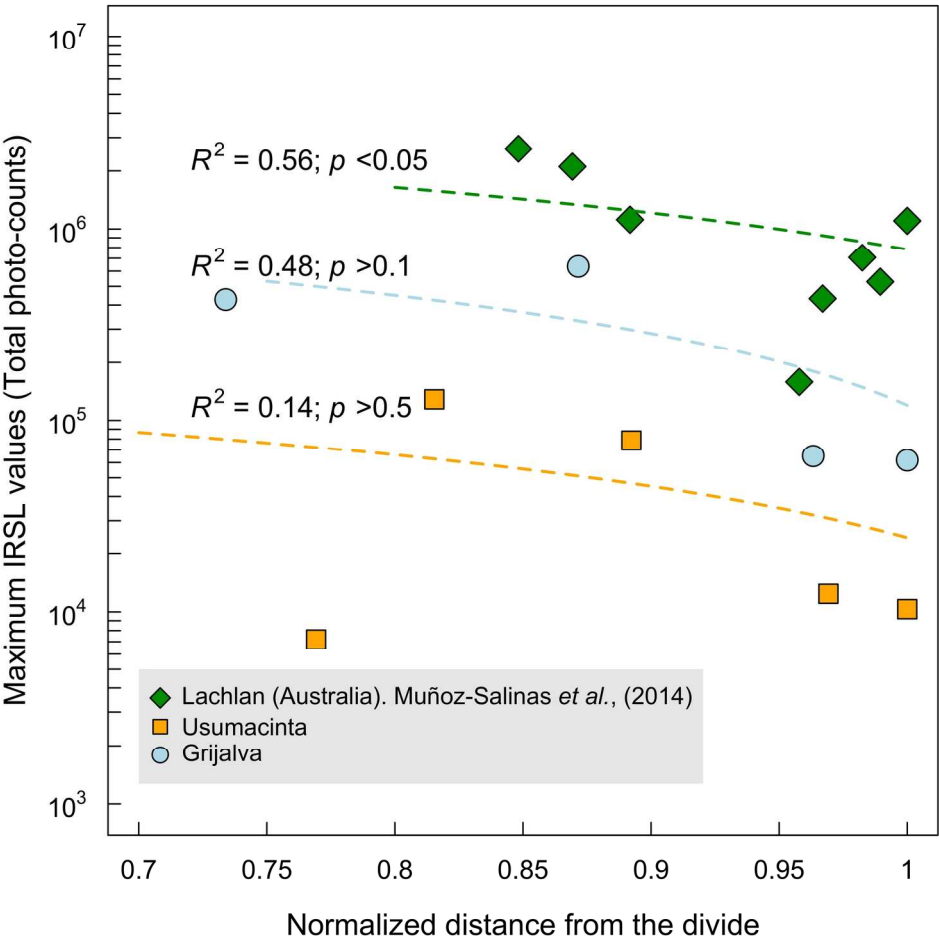


68x27mm (300 x 300 DPI)



296x428mm (300 x 300 DPI)





177x177mm (300 x 300 DPI)